Qiu, X., Tian, L., Wu, K., Benton, M. J., Sun, D., Yang, H., & Tong, J. (2019). Diverse earliest Triassic ostracod fauna of the non-microbialite-bearing shallow marine carbonates of the Yangou section, South China. *Lethaia*, *52*(4), 583-596. https://doi.org/10.1111/let.12332

Diverse earliest Triassic ostracod fauna from the non-microbialite-bearing shallow marine carbonates of the Yangou section in South China

XINCHENG QIU, LI TIAN, KUI WU, MICHAEL J. BENTON, DONGYING SUN, HAO YANG AND JINNAN TONG

Since diverse ostracod faunas in the immediate aftermath of the latest Permian mass extinction were mainly found within Permian-Triassic boundary microbialites (PTBMs), the idea of an ostracod "microbial related refuge" has been proposed. Here we report a diversified earliest Triassic ostracod fauna from the Yangou section in South China, where no PTBMs were deposited, providing evidence inconsistent with the "microbial related refuge" hypothesis. Meanwhile, a significant ostracod extinction was recorded, corresponding with the earliest Triassic mass extinction (ETME). This ETME of ostracods was associated with size increases and a length/height ratio (L/H) decrease, indicating varied evolutionary patterns of shape and size of ostracods through the Permian-Triassic (P-Tr) extinction events. Although the nature of these biotic changes is somewhat unclear, the temporally varied "refuge zone" scenario provides us a window to reconstruct the environmental dynamics of ecosystem changes during the P-Tr transition.

Key words: *Hollinella*, body size, mass extinction, refuge zone, recovery, marine ecosystem

Xincheng Qiu [qxch0309@163.com], Li Tian [tianlibgeg@163.com], Kui Wu [kuiwu@cug.edu.cn], Hao Yang [2003yanghao@163.com], Jinnan Tong* [jntong@cug.edu.cn], State Key Laboratory of Biogeology and Environmental Geology, China University of Geosciences, Wuhan, 430074, China; Li Tian [tianlibgeg@163.com], Michael J. Benton [glmjb@bristol.ac.uk], School of Earth Sciences, University of Bristol, BS8 1 RJ, UK; Dongying Sun [nancysun918@163.com], College of tourism and territorial resources, Jiujiang University, Jiujiang, 332005, China.* *Corresponding authors.

As one of the major components of the marine benthic ecosystem, ostracods were heavily affected by the Permian-Triassic (P-Tr) crisis, in which over 90% of marine invertebrate species and 70% of terrestrial animals went extinct (e.g. Erwin 1994; Benton & Twitchett 2003; Shen *et al*. 2011; Payne & Clapham 2012; Benton & Newell 2014). The extinction rates of the latest Permian ostracod faunas exceeded 70% and may be 100% in some localities (Crasquin & Forel 2014) during the major phase of the P-Tr crisis, corresponding to the latest Permian mass extinction (LPME) of Song *et al*. (2013).

Many researchers have attempted to explore survival and recovery patterns by studying well-preserved fossil faunas of the extinction aftermath in the Early Triassic (e.g. Twitchett *et al*. 2004; Benton *et al*. 2004, 2013; Song *et al*. 2011; Brayard *et al*. 2010, 2017; Hautmann *et al*. 2015; Godbold *et al*. 2017; Ji *et al*. 2017; Zhang *et al*. 2017). Ostracods have also attracted great research interest because of their wide habitat ranges and ecological significance (e.g. Wang 1978; Kozur 1991; Crasquin *et al*. 2007a, b; Yuan 2008; Crasquin & Forel 2014; Chu *et al*. 2015; Forel *et al*. 2015a). Dozens of publications have reported P-Tr ostracod faunas in various facies, including neritic clastic (Hao 1992), shallow carbonate (e.g. Crasquin *et al*. 2005, 2006, 2007b, 2018; Forel *et al*. 2009, 2013a, 2013b, 2015a, 2015b), and slope and deeper facies (Yuan *et al*. 2007; Crasquin *et al*. 2010).

The exceptionally high abundance and diversity of ostracods in Permian-Triassic boundary microbialites (PTBM) was thought to be evidence for a “microbial related refuge” scenario in the immediate aftermath of the LPME (Forel *et al*. 2009, 2012, 2013). However, herein we present a newly discovered diversified ostracod fauna in the earliest Triassic non-microbialite, shallow marine carbonates of the Yangou section, as a means of testing the “microbial related refuge” scenario. Meanwhile, temporal diversity and abundance changes as well as size variations are analyzed to

explore the impact on shallow marine ostracods of the second phase of the P-Tr crisis, the earliest Triassic mass extinction (ETME; identified by Song *et al*. (2013)). Furthermore, our quantitative data also show some inconsistent results with the newly established ontogeny model of *Hollinella lungcamensis* (Crasquin *et al*. 2018), providing additional evidence for systematic re-evaluation of *Hollinella*.

Geological setting and method

The Yangou section was located on the northern margin of the Yangtze Platform during the P-Tr transition (Fig. 1), in the eastern-most Paleotethys realm (Fig. 1). The studied P-Tr successions are composed of the Upper Permian Changxing Formation and Lower Triassic Daye Formation, with continuous deposition of carbonates (Fig. 2). The Changxing Formation is dominated by medium-thick bedded limestones, overlain by the Daye Formation and its thin-medium bedded limestones and muddy limestones. Two oolitic limestone beds were found at the base of the Daye Formation, implying shallow seawater level (Tian *et al*. 2014a, b). These lithologies and microfacies analyses suggest a platform–margin facies (Fig. 3; Tian *et al*. 2014a).

The study interval can be well constrained by other well studied P-Tr sections in South China, both lithologically and bio-stratigraphically (Song *et al*. 2012; Sun *et al*. 2012; Tian *et al*. 2014a, 2015), providing a solid stratigraphic basis for further palaeontological study and correlations. Ostracods and other fossils of the P-Tr successions in the study areas were initially reported by Zhu (1999), but the results were unreliable in the absence of fossil photographs and detailed descriptions. Renewed outcrop exposure for cement quarrying was bio-stratigraphically constrained at decimetre-level resolution (Fig. 3) using conodonts by Sun *et al*. (2012). Since then, foraminiferal

extinction (Tian *et al*. 2014b), carbon isotope variation (Song *et al*. 2012), facies and microfacies diagnoses (Tian *et al*. 2014a, 2015), elemental compositions (Li *et al*. 2017) and the carbonate diagenesis history (Li & Jones 2017) have been explored in detail in the Yangou study section.

Field sampling and bulk sample dissolution have been conducted for study of the ostracods and conodonts, as introduced in detail by Sun *et al*. (2012). Note that the acetic acid we used was at 10% concentration, and the use of dilute acid has ensured that dozens of exceptionally well-preserved specimens, like *Hollinella* (Fig. 4 A–H), were retained. All specimens are deposited in the collections of the State Key Laboratory of Biogeology and Environmental Geology, China University of Geosciences (Wuhan). The collections have been numbered in this way: LY(section name)**(bed number)+**(sampling number)i**(ostracod specimen number). In all specimens we measured the length (L) and height (H) for quantitative size analyses. Size variations are shown in plotted boxes including length, height, Log(length×height). The specimens belonging to *Hollinella* were plotted in a Height/Length diagram.

Results and Discussion

In total, 238 well preserved ostracod specimens were found from nine sampling horizons (Fig. 3). These ostracods are all from the wackestones of the Daye Formation (Fig. 2B–C; diagnosed as restricted inner-shelf shallow marine facies by Tian *et al.* 2014a), that lack microbial related structures in the matrix (Fig. 2B–C). In total, 34 species belonging to eight genera of ostracods have been identified and measured (Figs. 4–5; Table 1).

New materials for Hollinella *classification*

89

90 The ostracod *Hollinella* is often present in many P-Tr boundary sections globally (Crasquin et *al*.
91 2018). However, especially for *Hollinella tingi*, a proposed bio-stratigraphical index for the P-Tr
92 boundary (Kozur 1985), the systematic classification is confused (Crasquin *et al*. 2018).
93 Morphological variations of *Hollinella* specimens are presented here as a means of testing aspects of
94 their systematic classification. From these samples, we identify three morphotypes, termed sp. 1–3
95 here.

96 *Hollinella* sp. 1 is characterized by its smooth, spineless surface, rounded anterior and posterior
97 borders, straight dorsal margin and two distinct nodules, belonging either to *H. tingi* (Patte 1935) or
98 *H. panxiensis* (Wang 1978), according to the descriptions of these two species by Wang (1978). In
99 the review of the history of *H. tingi* by Crasquin *et al*. (2018), it is very difficult to trace the real *H.*
100 *tingi* from the indefinite descriptions by Patte (1935) and Hou (1954). Crasquin *et al*. (2018)
101 interpreted all specimens assigned to *H. tingi* to be *H. panxiensis*, since Wang (1978) established *H.*
102 *panxiensis* with clear descriptions and he indicated differences from *H. tingi*. However, a long dorsal
103 spine and an obtuse spine reaching over the dorsal margin were noted for *H. panxiensis* and *H. tingi*,
104 respectively, by Wang (1978). In the absence of such spines in our *Hollinella* sp. 1 (Fig. 4A–D), it
105 cannot be either *H. panxiensis* or *H. tingi*.

106 *Hollinella* sp. 2 is identified on similar morphological features as *H.* sp. 1, but the occurrence of
107 spinous shells (Fig. 4E–H) suggests it may belong to the species *H. lungcamensis* which was
108 established by Crasquin *et al*. (2018). These authors proposed an ideal ontogenetic model for its
109 growth stage and sexual dimorphism, and if this ontogeny model is correct, the juveniles (spinous)
110 should be smaller than the adults (with velum), but their H/L ratios fail to show a clear boundary

between juveniles and adults (see Crasquin *et al*. 2018, fig. 5). Furthermore, our body size measurements show that *H*. sp. 2 should be an independent new taxon based on its wide size distributions (Fig. 6; varying from very small to very large) and coexistence of velum and spinous shells (Fig. 4E–H).

According to the classification in Crasquin *et al*. (2018), our *Hollinella* sp. 3 should be female adults of *H*. *lungcamensis* because of the occurrence of a velum and a few spines on the lobes (see Crasquin *et al*. 2018, fig. 2, fig. 5A–H). Unfortunately, the actual body size measurements of our specimens fail to show that *H*. sp. 2 (interpreted as juveniles of *H*. *lungcamensis* by Crasquin *et al*. (2018)) are smaller than *H*. sp. 3 (Fig. 6). The length, positions and spaces of these spines on our *H*. sp. 3 are significantly lower than in our *H*. sp. 2. Additionally, there is an obtuse "spine" reaching over the dorsal margin in our *H*. sp. 3 (Fig. 4I–L), making our *H*. sp. 3 very similar to *H*. *capacilacuna*. However, the distinct spinous posterior border was not noted in the description of *H*. *capacilacuna* (Wang 1978), and a distinct arcuate ridge in the ventral lobe, around the tumours, on most specimens, has also been observed (Fig. 4A–C), neither of which was noted in the description of *H*. *capacilacuna* by Wang (1978). Thus, we cannot confidently assign our *H*. sp. 3 to either *H*. *capacilacuna* or a new species.

In addition, the H/L ratios imply a potential ontogenetic link between these "two species", *H*. sp. 1 and *H*. sp. 3 (Fig. 6). This means that our *H*. sp. 1 and *H*. sp. 3 might be juvenile and adult of a single species, respectively. In the ontogeny model of *H*. *camoni*, distinct spines occurred on the posterior margin in the adults, while the shell margin of young juveniles looks smooth, with extremely tiny spines (Bless 1968). Possible tiny spines on the margin can also be observed on some specimens of our *H*. sp. 3 (Fig. 4I–L), supporting our assumed ontogenetic relationships between *H*.

133 sp. 1 and *H*. sp. 3.

134

135 *Earliest Triassic ostracod extinction and associated size variations*

136 Although the absence of pre-LPME specimens precludes the correlation of the LPME extinction
137 pattern with other sections, the succession of earliest Triassic specimens shows a distinct extinction
138 at the top of the *H. parvus* Zone (between LY4 with LY5, see Table 1), corresponding to the ETME
139 (Fig. 7). Song *et al*. (2013) constrained the ETME to the *Isarcicella staeschei* Zone, as the terminal
140 event of the P-Tr crises. Precise conodont biozonations of the Yangou study section show that the
141 ETME occurred at the top of the *H. parvus* Zone, implying a potential earlier ETME at Yangou (Fig.
142 3; Sun *et al*. 2012). However, because no conodont has been obtained from samples between LY4
143 and LY6 (Sun *et al*. 2012), it is likely that the true lowest occurrence of *Isarcicella staeschei* might
144 be lower than LY5, dating the ETME at Yangou to the *Isarcicella staeschei* Zone.

145 Differing from the observed Lilliput effect of ostracods during the LPME (Chu *et al*. 2015; Forel
146 *et al*. 2015a; Forel & Crasquin 2015), we find that sizes (Length, Height and Length*Height) show a
147 gradual increase across the ETME at Yangou (Fig. 8A). Possible reasons could be either or both: 1)
148 body size had been reduced to a very low level in the LPME by severe environmental devastation,
149 and the following environmental oxygenation contributed to rapid reoccupation and size increase (He
150 *et al*. 2017); or 2) Cope's rule (e.g. Hone & Benton 2005; Benson *et al*. 2017) applied to the
151 surviving populations (*Hollinella* sp. 1) and new-comers (*Hollinella* sp. 2 and *Hollinella* sp. 3) in the
152 aftermath of the ETME. Although numerous studies just reported size reduction during the P-Tr mass
153 extinction (e.g. ostracods: Chu *et al*. 2015; Forel *et al*. 2015; brachiopods: He *et al*. 2010, 2015;
154 conodonts: Luo *et al*. 2008; foraminifera: Song *et al*. 2011; and see Twitchett, 2007), a body size

increase across the second extinction phase has been noted in brachiopods (Wu *et al*. 2018) and ostracods (this study), and further such high-resolution studies are required to decipher these unique biotic response dynamics in mass extinctions.

Size variations of ostracods might be biased by the dominance of adults/juveniles (Forel et al. 2015a), but the results cannot be further tested for the problematic ontogenetic models we noted above. Fossil size changes could indicate ecosystem stress. Payne et al. (2004) stated that the recovery in the aftermath of the LPME lasted over 5 Myr, based on the delayed size increase of gastropods in the Middle Triassic. Brayard et al. (2010) argued that the rapid size increase of gastropods in the Smithian (about 1 Myr after LPME) indicated rapid ecosystem recovery. However, the transient ostracod size increase we observe in the *Hindeodus parvus* Zone did not result from rapid ecosystem recovery, but the domination by *Hollinella* suggests they were opportunistic assemblages rather than recovered Mesozoic assemblages (Crasquin *et al.* 2007b). Such dynamics have also been applied to explain the synchronous brachiopod size increase in deeper settings by Wu *et al.* (2018). Additionally, temporary environmental improvements during the *H. parvus* Zone (details below) also contributed to this assemblage replacement and the associated size increase.

Chu *et al*. (2015) reported a reduction in L/H ratios for ostracods during the LPME. Forel & Crasquin (2015) argued that the differential extinction of ostracods with high L/H ratios provides a new proxy together with body size (length, height and volume) to explore the nature of extinctions. On the other hand, our results suggest that the L/H ratio decreased during the ETME at Yangou (Fig. 8B; the slight increase in LY7 is meaningless, as it is based on only one measurement). The measured L/H ratio distributions in *Hollinella*, *Bairdia* and *Acratia* show smaller L/H ratios than other genera (Fig. 9). Indeed, the post-ETME assemblages are dominated by *Hollinella* with very

177 few *Bairdia* (Fig. 7), indicating potentially higher survival probability for the low L/H specimens.
178 However, *Acratia* went extinct during the ETME despite its low L/H, implying additional unclear
179 extinction/survival dynamics.
180
181 *Reconsideration of the "microbial related refuge" scenario for ostracods during the P-Tr transition*
182 The high diversity and abundance of the ostracod faunas in the *H. parvus* Zone presented here
183 suggest that Yangou is a potential earliest Triassic favourable metazoan habitat (refuge). Such an
184 occurrence of ostracods in Permian-Triassic transitional beds (PTTB) is notable when compared to
185 other settings globally (Table 2). At the P-Tr boundary GSSP Meishan section, although the
186 abundance and diversity in Bed 27 is lower than in the strata below Bed 24e, ostracods did not go
187 totally extinct until Bed 30 (Crasquin *et al*. 2010; Forel *et al*. 2011). In the Dajiang section in South
188 China, ostracods are abundant in shelly layers within PTBMs (Forel *et al*. 2009; Forel 2012), which
189 were most recently constrained to belong to the *H. parvus* Zone (Jiang *et al*. 2014). Similar high
190 diversity and abundance of ostracods within PTBMs have also been reported in the Chongyang and
191 Laolongdong sections on the Yangtze Platform, the Lung Cam section in Vietnam, and the Cürük
192 Dag section in Turkey (Crasquin & Kershaw 2005; Liu *et al*. 2010; Crasquin *et al*. 2018). Including
193 the Yangou section, ostracods are also abundant and diversified in the *H. parvus* Zone in some
194 oolite-bearing P-Tr successions, such as Bulla in Italy and Balvany in Hungary as well as the Elikah
195 River section (Crasquin *et al*. 2004; Forel *et al*. 2013a, 2015b), from the latest Permian to earliest
196 Triassic. Earliest Triassic ostracod faunas have also been found in the *Clarkina meishanensis*
197 Zone–*H. parvus* Zone equivalent strata in siliceous P-Tr successions in Guizhou and Yunnan (Wang
198 1978; Hao 1992; Yu *et al*. 2010; Chu *et al*. 2016). It is worth noting that all these mentioned sections

were in shallow water facies.

The "microbial related refuge" proposed by Forel *et al*. (2009) is somewhat ambiguous in terms of the complicated ecological interactions between metazoans and microbialites. Thrombolites are characterized by a mixed bacterial-metaphyte ecosystem of greater complexity than the microbial-dominated biotas of stromatolitic mats in the modern Bahamian Platform (Planavsky & Ginsburg 2009; Tarhan *et al*. 2013). The thromobolites of PTBMs always have a much greater metazoan fossil content (e.g. Yang *et al*. 2011; Tang *et al*. 2017; Tian *et al*. 2018) than coeval stromatolitic mats, which tend to contain few marine invertebrates (e.g. Adachi *et al*. 2017; Fang *et al*. 2017). Shelly layers, dominated by ostracods and gastropods, are very common in PTBMs (e.g. Kershaw *et al*. 2012). However, these shelly layers or shell lenses are often preserved between the PTBMs, hydrodynamically accumulated in troughs between the microbial domes (Hautmann *et al*. 2015), and showing no evidence that metazoans lived in these microbial domes.

Abundant diversified ostracod faunas of the earliest Triassic might be biotic responses to a sharp break in environmental devastation in the *H. parvus* Zone. The high abundance and diversity of ostracod faunas within PTBMs were interpreted as evidence of habitable conditions, which were provided by PTBMs as potential refuges (Forel *et al*. 2009, 2013). The abundances of ostracods within PTBMs are higher than in other facies, but the diversities of PTTB of shallow successions are equivalent (Table 2). Therefore, the synchronous intensive and extensive occurrences of ostracods in non-PTBM successions (e.g. Yangou and Bulla) cannot be explained by the microbialite-refuge scenario. Further, reliable evidence for ostracod-grazing microbes is also absent from PTBMs. A high oxygen level for microbial blooms in PTBMs was inferred (Forel *et al*. 2009, 2013), despite the evidence for dysoxic (not fully oxygenated) conditions in PTBMs (Brennecka *et al*. 2011; Liao *et al*.

2017; Xiao *et al*. 2018).

Thus, we prefer to accept the idea of a temporally synchronous "shallow-water refuge" in various facies rather than the microbialite-related "refuge". Song *et al*. (2014) proposed temporal "refuge zone" variations from the latest Permian to Middle Triassic, showing a clear refuge zone expansion in the *H*. *parvus* Zone, as the potential dynamic for a diversified fauna (including ostracods) between the LPME and the ETME (Song *et al*. 2013). Recent studies have suggested that there is little evidence for conditions favourable to metazoans in the *H*. *parvus* Zone, such as an oxygenation event (Bond & Wignall 2010; Loopes *et al*. 2013; Li *et al*. 2016; Xiao *et al*. 2018), paused temperature rise (Joachimski *et al*. 2012) or moderate pH (Clarkson *et al*. 2015).

Following the rapidly expanded refuge zone during the time of the *H*. *parvus* Zone, the ostracod extinction at the ETME was likely caused by synchronous lethal environmental crises, including temperature rise (Joachimski *et al*. 2012), euxinia expanding into the photic zone (Grice *et al*. 2005; Xie *et al*. 2017), ocean acidification (Clarkson *et al*. 2015), carbonate factory overturns (Tian *et al*. 2015) and others. Though the ecological dynamics for survival selectivity of species with low L/H ratios and non-Lilliput effects among ostracods through the ETME uncovered at Yangou are unclear, further eco-physiological research is needed to decipher these unique biotic responses to environmental devastation.

Conclusions

Following the results and discussion presented above, four important conclusions are:

1) The new materials of the ostracod genus *Hollinella* show that the current identification and nomenclature of some species is unclear;

2) A distinct ostracod extinction horizon is recorded in the earliest Triassic (latest *Hindeodus parvus* Zone or earliest *Isarcicella staeschei* Zone), associated with increasing body size and reducing L/H ratio;
3) The diverse ostracod fauna in the Yangou section suggests that ostracods occurred in various carbonate facies, not only PTBMs, during the pause between the LPME and ETME, implying a temporal "refuge zone" in shallow marine settings, rather than the scenario of spatial refuge related to PTBMs;
4) Both the diverse ostracod fauna in the *Hindeodus parvus* Zone and ETME, and related size variations uncovered in this study, correspond to rapid ecological and environmental changes, providing new biotic responses (rapid recovery and increase of size) for future mass extinction studies.

Acknowledgements

We thank Prof. Zhongqiang Chen, Dr. Aihua Yuan, and Junyu Wan for helpful advice on taxonomic identification and technical support of SEM photography. Constructive editing and comments from Dr Alan Owen, Dr Junjun Song and Dr Paul Wignall are appreciated. This study was supported by the National Science Foundation of China (grant nos. 41530104, 41562002, 41602204 and 41661134047), the State Key Laboratory of Biogeology and Environmental Geology (GBL11605) and it also benefited from the sponsored international exchange programme to L.T. (by China Postdoctoral Science Foundation). Funded also by NERC BETR grant NE/P013724/1 to M.J.B. It is also a contribution to IGCP 630.

References

Adachi, N., Asada, Y., Ezaki, Y. & Liu, J. 2017: Stromatolites near the Permian-Triassic boundary in Chongyang, Hubei Province, South China: A geobiological window into palaeo-oceanic fluctuations following the end-Permian extinction. *Palaeogeography, Palaeoclimatology, Palaeoecology 475*, 55–69.

Algeo, T.J., Chen, Z.Q., Fraiser, M.L., & Twitchett, R.J. 2011: Terrestrial-marine teleconnections in the collapse and rebuilding of Early Triassic marine ecosystems. *Palaeogeography, Palaeoclimatology, Palaeoecology 308*, 1–11.

Benson, R.S., Hunt, G., Carrano, M.T. & Campione, N. 2017: Cope's rule and the adaptive landscape of dinosaur body size evolution. *Palaeontology 61*, 13–48.

Benton, M.J. & Newell, A.J. 2014: Impacts of global warming on Permo–Triassic terrestrial ecosystems. *Gondwana Research 25*, 1308–1337.

Benton, M.J., Tverdokhlebov, V.P., & Surkov, M.V. 2004: Ecosystem remodelling among vertebrates at the Permian–Triassic boundary in Russia. *Nature 432*, 97–100.

Benton, M.J., & Twitchett, R.J. 2003: How to kill (almost) all life: the end-Permian extinction event. *Trends in Ecology & Evolution 18*, 358–365.

Benton, M.J., Zhang, Q., Hu, S., Chen, Z.Q., Wen, W., Liu, J., Huang, J., Zhou, C., Xie, T., Tong, J. & Choo, B. 2013: Exceptional vertebrate biotas from the Triassic of china, and the expansion of marine ecosystems after the permo-triassic mass extinction. *Earth-Science Reviews 125*, 199–243.

Bond, D.P.G. & Wignall, P.B. 2010: Pyrite framboid study of marine Permian–Triassic boundary sections: A complex anoxic event and its relationship to contemporaneous mass extinction. *Geological Society of America Bulletin 122*, 1265–1279.

Bless, M.J.M. 1968: On two hollinid ostracode genera from the Upper Carboniferous of northwestern Spain. *Leidse Geologische Mededelingen 43*, 157–212.

Brayard, A., Nutzel, A., Stephen, D.A., Bylund, K.G., Jenks, J. & Bucher, H. 2010: Gastropod evidence against the Early Triassic Lilliput effect. *Geology 38*, 147–150.

Brayard, A., Krumenacker, L.J., Botting, J.P., Jenks, J.F., Bylund, K.G., Fara, E., Vennin, E., Olivier, N., Goudemand, N. & Saucède, T. 2017: Unexpected Early Triassic marine ecosystem and the rise of the Modern evolutionary fauna. *Science Advances 3*, e1602159.

Brennecka, G.A., Herrmann, A.D., Algeo, T.J. & Anbar, A.D. 2011: Rapid expansion of oceanic anoxia immediately before the end–Permian mass extinction. *Proceedings of the National Academy of Sciences 108*, 17631–17634.

Burgess, S.D., Bowring, S. & Shen, S.Z. 2014: High-precision timeline for Earth's most severe extinction. *Proceedings of the National Academy of Sciences (U.S.A.) 11*, 3316–3321.

Chu, D., Tong, J., Song, H., Benton, M. J., Song, H., Yu, J., Qiu, X., Huang, Y. & Tian, L. 2015: Lilliput effect in freshwater ostracods during the Permian–Triassic extinction. *Palaeogeography, Palaeoclimatology, Palaeoecology 435*, 38–52.

Chu, D., Yu, J., Tong, J., Benton, M.J., Song, H., Huang, Y. Song, T. & Tian, L. 2016: Biostratigraphic correlation and

mass extinction during the Permian–Triassic transition in terrestrial–marine siliciclastic settings of South China. *Global and Planetary Change 146*, 67–88.

Clarkson, M.O., Kasemann, S.A., Wood, R.A., Lenton, T.M., Daines, S.J., Richoz, S., Ohnemueller, F., Meixner, A., Poulton, S.W. & Tipper, E.T. 2015: Ocean acidification and the Permo–Triassic mass extinction. *Science 348*, 229–232.

Crasquin, S., Marcoux, J., Angiolini, L., Richoz, S., Nicora, A., Baud, A., & Bertho, Y. 2004: Palaeocopida (Ostracoda) across the Permian–Triassic events: New data from southwestern Taurus (Turkey). *Journal of Micropalaeontology 23*, 67–76.

Crasquin, S., Vaslet, D. & Nindre, Y.M.L. 2005: Ostracods as markers of the Permian/Triassic boundary in the Khuff Formation of Saudi Arabia. *Palaeontology* 48, 853–868.

Crasquin, S. & Kershaw, S. 2005: Ostracod fauna from the Permian–Triassic boundary interval of South China (Huaying Mountains, eastern Sichuan Province): palaeoenvironmental significance. *Palaeogeography, Palaeoclimatology, Palaeoecology 217*, 131–141.

Crasquin, S., Galfetti, T., Bucher, H. & Brayard, A. 2006: Palaecological changes after the end–Permian mass extinction: Early Triassic ostracods from northwestern Guangxi Province, South China. *Rivista Italiana di Paleontologia e Stratigrafia 112*, 55–75.

Crasquin, S., Galfetti, T., Bucher, H., Kershaw, S. & Feng, Q. 2007a: Ostracod recovery in the aftermath of the Permian–Triassic crisis: Palaeozoic–Mesozoic turnover. *Hydrobiologia 585*, 13–27.

Crasquin, S., Shen, S.Z., Li, W.Z. & Cao, C.Q. 2007b: Ostracods from the Lopingian and Permian-Triassic boundary beds at the Gyanyima section in southwestern Tibet, China. *Palaeoworld 16*, 222–232.

Crasquin, S., Perri, M.C., Nicora, A. & Wever, P.D. 2008: Ostracods across the permian-triassic boundary in western Tethys: the Bulla parastratotype (southern Alps, Italy). *Rivista Italiana di Paleontologia e Stratigrafia 114*, 233–262.

Crasquin, S., Forel, M., Feng, Q., Yuan, A. Baudin, F. & Collin, P. 2010: Ostracods (Crustacea) through the Permian–Triassic boundary in South China: the Meishan stratotype (Zhejiang Province). *Journal of Systematic Palaeontology 8*, 331–370.

Crasquin, S. & Forel, M. 2014: Ostracods (Crustacea) through Permian–Triassic events. *Earth–Science Reviews 137*, 52–64.

Crasquin, S., Forel, M., Yuan, A., Nestell, G. & Nestell, M. 2018: Species of Hollinella (Palaeocopida: Ostracoda: Crustacea) as stratigraphical indices of the Late Permian–Early Triassic post–extinction interval. *Journal of Systematic Palaeontology 16*, 213–224.

Erwin, D.H. 1994: The Permo–Triassic extinction. *Nature 367*, 231–236.

Fang, Y., Chen, Z.Q., Kershaw, S., Yang, H. & Luo, M. 2017: Permian-Triassic boundary microbialites at Zuodeng Section, Guangxi Province, South China: Geobiology and palaeoceanographic implications. *Global and Planetary Change 152*, 115–128.

Farabegoli, E., Perri, M.C. & Posenato, R. 2007: Environmental and biotic changes across the Permian-Triassic boundary

in western Tethys: The Bulla parastratotype, Italy. *Global and Planetary Change 55*, 109–135.

Forel, M.B., Crasquin, S., Kershaw, S., Feng, Q.L. & Collin, P.Y. 2009: Ostracods (Crustacea) and water oxygenation in the earliest Triassic of south China: implications for oceanic events at the end–Permian mass extinction. *Journal of the Geological Society of Australia 56*, 815–823.

Forel, M.B. & Crasquin, S. 2011: Lower Triassic ostracods (Crustacea) from the Meishan section, Permian–Triassic boundary GSSP (Zhejiang Province, South China). *Journal of Systematic Palaeontology 9*, 455–466.

Forel, M.B. 2012: Ostracods (Crustacea) associated with microbialites across the Permian–Triassic boundary in Dajiang (Guizhou Province, South China). *European Journal of Taxonomy 19*, 1–34.

Forel, M.B., Crasquin, S., Kershaw, S. & Collin, P. 2013a: In the aftermath of the end–Permian extinction: the microbialite refuge? *Terra Nova 25*, 137–143.

Forel, M.B., Crasquin, S., Hips, K., Kershaw, S., Collin, P. Y. & Haas, J. 2013b: Biodiversity evolution through the Permian—Triassic boundary event: Ostracods from the Bükk Mountains, Hungary. *Acta Palaeontologica Polonica 58*, 195–219.

Forel, M.B. & Crasquin, S. 2015: Comment on the Chu et al. paper "Lilliput effect in freshwater Ostracods during the Permian–Triassic extinction" [Palaeogeography, Palaeoclimatology, Palaeoecology 435 (2015): 38–52]. *Palaeogeography, Palaeoclimatology, Palaeoecology 440*, 860–862.

Forel, M.B., Crasquin, S., Chitnarin, A., Angiolini, L. & Gaetani, M. 2015a: Precocious sexual dimorphism and the Lilliput effect in Neo–Tethyan Ostracoda (Crustacea) through the Permian–Triassic boundary. *Palaeontology 58*, 409–454.

Forel, M.B., Crasquin, S., Hips, K., Kershaw, S., Collin, P.Y. & Haas, J. 2015b: Biodiversity Evolution Through the Permian–Triassic Boundary Event: Ostracods from the Bükk Mountains, Hungary. *Acta Palaeontologica Polonica 58*, 195–219.

Godbold, A., Schoepfer, S., Shen, S., Henderson, C.M., Godbold, A., Schoepfer, S., Shen, S., Henderson, C.M., Godbold, A. & Schoepfer, S. 2017: Precarious ephemeral refugia during the earliest Triassic. *Geology 45*, 607–610.

Grice, K., Cao, C., Love, G.D., Böttcher, M. E., Twitchett, R. J., Grosjean, E., Summons, R. E., Turgeon, S. C., Dunning, W. & Jin, Y. 2005: Photic zone euxinia during the Permian–Triassic superanoxic event. *Science 307*, 706–709.

Hao, W. 1992: Early Triassic ostracods from Guizhou. *Acta Micropalaeontologica Sinica 9*, 37–44. [In Chinese with English abstract.]

Hautmann, M., Bagherpour, B., Brosse, M., Frisk, Å., Hofmann, R., Baud, A., Nützel, A., Goudemand, N. & Bucher, H. 2015: Competition in slow motion: the unusual case of benthic marine communities in the wake of the end–Permian mass extinction. *Palaeontology 58*, 871–901.

He, W.H., Twitchett, R.J., Zhang, Y., Shi, G.R., Feng, Q.L., Yu, J.X., Wu, S.B. & Peng, X.F. 2010: Controls on body size during the Late Permian mass extinction event. *Geobiology 8*, 391–402.

He, W.H., Shi, G.R., Twitchett, R.J., Zhang, Y., Zhang, K.X., Song, H.J., Yue, M.L., Wu, S.B., Wu, H.T., Yang, T.L. & Xiao, Y.F. 2015: Late Permian marine ecosystem collapse began in deeper waters: evidence from brachiopod diversity and body size changes. *Geobiology 13*, 123–138.

He, W., Shi, G., Xiao, Y., Zhang, K., Yang, T., Wu, H., Zhang, Y., Chen, B., Yue, M., Shen, J., Wang, Y., Yang, H. & Wu, S. 2017: Body-size changes of latest Permian brachiopods in varied palaeogeographic settings in South China and implications for controls on animal miniaturization in a highly stressed marine ecosystem. *Palaeogeography, Palaeoclimatology, Palaeoecology 486*, 33–45.

Hone, D.W.E. & Benton, M.J. 2005: The evolution of large size: how does Cope's Rule work. *Trends in Ecology & Evolution 20*, 4–6.

Hou, Y. 1954: Some Lower Permian ostracods from Western Hupei. *Acta Palaeontologica Sinica 2*, 227–266. [In Chinese with English abstract.]

Ji, C., Tintori, A., Jiang, D.Y. & Motani, R. 2017: New species of Thylacocephala (Arthropoda) from the Spathian (Lower Triassic) of Chaohu, Anhui Province of China. *PalZ 91(2)*, 171–184.

Jiang, H., Lai, X., Sun, Y., Wignall, P.B., Liu, J. & Yan, C. 2014: Permian–Triassic Conodonts from Dajiang (Guizhou, South China) and Their Implication for the Age of Microbialite Deposition in the Aftermath of the End–Permian Mass Extinction. *Journal of Earth Science 25*, 413–430.

Joachimski, M.M., Lai, X., Shen, S., Jiang, H., Luo, G., Chen, B., Chen, J. & Sun, Y. 2012: Climate warming in the latest Permian and the Permian–Triassic mass extinction. *Geology 40*, 195–198.

Kershaw, S., Crasquin, S., Li, Y., Collin, P.Y., Forel, M.B., Mu, X., Baud, A., Wang, Y., Xie, S. & Maurer, F. 2012: Microbialites and global environmental change across the Permian-Triassic boundary: a synthesis. *Geobiology 10*, 25–47.

Kozur, H. 1971: Die Bairdiacea der Trias. Teil 3: Einige neue Arten triassischer Bairdiacea und Bemerkungen zur Herkunft der Macrocyprididae (Cypridacea). *Geologisch Paläontologische Mitteilungen Innsbruck 1*, 1–18.

Kozur, H. 1991: Permian deep–water ostracods from Sicily (Italy). Part 2: Biofacial evaluation and remarks to the Silurian to Triassic paleopsychrospheric ostracods. *Geologisch–Paläontologische Mitteilungen Innsbruck 3*, 25–38.

Li, G., Wang, Y., Shi, G., Liao, W. & Yu L. 2016: Fluctuations of redox conditions across the Permian-Triassic boundary-New evidence from the GSSP section in Meishan of South China. *Palaeogeography, Palaeoclimatology, Palaeoecology 448*, 48–58.

Li, R., Jones, B. 2017: Diagenetic overprint on negative $\delta^{13}C$ excursions across the Permian/Triassic boundary: A case study from Meishan section, China. *Palaeogeography, Palaeoclimatology, Palaeoecology 468*, 18–33.

Li, Y., Zhao, L., Chen, Z.Q., Algeo, T.J., Cao, L. & Wang, X. 2017: Oceanic environmental changes on a shallow carbonate platform (Yangou, Jiangxi Province, South China) during the Permian–Triassic transition: Evidence from rare earth elements in conodont bioapatite. *Palaeogeography, Palaeoclimatology, Palaeoecology 486*, 6–16.

Liao, W., Bond, D.P.G., Wang, Y., He, L., Yang, H., Weng, Z. & Li, G. 2017: An extensive anoxic event in the Triassic of the South China Block: A pyrite framboid study from Dajiang and its implications for the cause(s) of oxygen depletion. *Palaeogeography, Palaeoclimatology, Palaeoecology 486*, 86–95.

Liu, H., Wang, Y., Yuan, A., Yang, H., Song, H. & Zhang, S. 2010: Ostracod fauna across the Permian–Triassic boundary at Chongyang, Hubei Province, and its implication for the process of the mass extinction. *Science China Earth Sciences 53*, 810–817.

Loope, G.R., Kump, L.R. & Arthur, M.A. 2013: Shallow water redox conditions from the Permian–Triassic boundary microbialite: The rare earth element and iodine geochemistry of carbonates from Turkey and South China. *Chemical Geology 351*, 195–208.

Luo, G., Lai, X., Shi, G. R., Jiang, H., Yin, H., Xie, S., Tong, J., Zhang, K., He, W. & Wignall, P. B. 2008: Size variation of conodont elements of the Hindeodus–Isarcicella clade during the Permian–Triassic transition in South China and its implication for mass extinction. *Palaeogeography, Palaeoclimatology, Palaeoecology 264*, 176–187.

Patte, E. 1935. Glanes préhistoriques dans les Balkans. Pierres à cupules. *Bulletin De La Société Préhistorique De France 32*, 221–244.

Payne, J.L., Lehrmann, D.J., Wei, J.Y., Orchard, M.J., Schrag, D.P. & Knoll, A.H. 2004: Large perturbations of the carbon cycle during recovery from the end-Permian extinction. *Science 23*, 506–509.

Payne, J.L. & Clapham, M.E. 2012: End–Permian Mass Extinction in the Oceans: An Ancient Analog for the Twenty–First Century? *Annual Review of Earth & Planetary Sciences 40*, 89–111.

Planavasky, N. & Ginsburg, R.N., 2009: Taphonomy of Modern Bahamian Microbialites. *Palaios 24*, 5–17.

Shen, S.Z., Crowley, J.L., Wang, Y., Bowring, S.A., Erwin, D.H., Sadler, P.M., Cao, C.Q., Rothman, D.H., Henderson, C. M. & Ramezani, J. 2011: Calibrating the end–Permian mass extinction. *Science 334*, 1367–1372.

Shi, C.G. & Chen D.Q. 1987: The Changhsingian ostracodes from Meishan, Changxing, Zhejiang. *Stratigraphy and Palaeontology of Systemic Boundaries in China; Permian and Triassic Boundary 5*, 23–80. [In Chinese with English abstract.]

Song, H.J., Wignall, P.B., Chen, Z.Q., Tong, J.N., Bond, D.P.G., Lai, X.L., Zhao, X.M., Jiang, H.S., Yan, C.B., Niu, Z.J., Chen, J., Yang, H. & Wang, Y.B. 2011: Recovery tempo and pattern of marine ecosystems after the end-Permian mass extinction. *Geology 39(8)*, 739–742.

Song, H.J., Tong, J.N., Xiong, Y., Sun, D.Y., Tian, L. & Song, H.Y. 2012: The large increase of δ^{13}Ccarb-depth gradient and the end-Permian mass extinction. *Science China: Earth Science 55*, 1101–1109.

Song, H.J., Wignall, P.B., Tong, J.N. & Yin, H.F. 2013: Two pulses of extinction during the Permian–Triassic crisis. *Nature Geoscience 6*, 52–56.

Song, H.J., Wignall, P.B., Chu D.L., Sun, D.Y., Song, H.Y., He, W.H. & Tian, L. 2014: Anoxia/high temperature double whammy during the Permian–Triassic marine crisis and its aftermath. *Scientific Reports 4*, srep04132.

Sun, D.Y., Tong, J.N., Xiong, Y.L., Tian, L. & Yin, H.F. 2012: Conodont Biostratigraphy and Evolution across Permian–Triassic Boundary at Yangou Section, Leping, Jiangxi Province, South China. *Journal of Earth Science 23*, 311–325.

Tarhan, I.G., Planavsky, N.J., Laumer, C.E., Stolz, J.E. & Reid, R.P. 2013: Microbial mat controls on infaunal abundance and diversity in modern marine microbialites. *Geobiology 11*, 485–497.

Tang, H., Kershaw, S., Liu, H., Tan, X.C., Li, F., Hu, G., Huang, C., Wang, L.C., Lian, C.B., Li, L. & Yang, X.F. 2017: Permian-Triassic boundary microbialites (PTBMs) in southwest China: implications for paleoenvironment reconstruction. *Facies 63(1)*, 2.

Tian, L., Tong, J., Sun, D., Xiong, Y., Wang, C., Song, H., Song, H. & Huang, Y. 2014a: The microfacies and

sedimentary responses to the mass extinction during the Permian–Triassic transition at Yangou Section, Jiangxi Province, South China. *Science China Earth Sciences 57*, 2195–2207.

Tian, L., Tong, J., Song, H., Liang, L., Yang, L., Song, H., Wang, C., Zhao, X. & Sun, D. 2014b: Foraminiferal evolution and formation of oolitic limestone near Permian–Triassic boundary at Yangou Section, Jiangxi Province. *Earth Science 39*, 1473–1486. [In Chinese with English abstract.]

Tian, L., Tong, J., Bottjer, D., Chu, D., Liang, L., Song, H. & Song, H. 2015: Rapid carbonate depositional changes following the Permian–Triassic mass extinction: Sedimentary evidence from South China. *Journal of Earth Science 26*, 166–180.

Tian, L., Tong, J.N., Xiao, Y.F., Benton, M.J., Song, H.Y., Song, H.J., Liang, L., Wu, K. & Chu, D.L. 2018: Environmental instability prior to end-Permian mass extinction reflected in biotic and facies changes on shallow carbonate platforms of the Nanpanjiang Basin (South China). *Palaeogeography, Palaeoclimatology, Palaeoecology*, in press. Doi: 10.1016/j.palaeo.2018.05.011.

Twitchett, R.J., Krystyn, L., Baud, A., Wheeley, J. R. & Richoz, S. 2004: Rapid marine recovery after the end–permian mass–extinction event in the absence of marine anoxia. *Geology 32*, 805–808.

Twichett, R.J. 2007: The Lilliput effect in the aftermath of the end-Permian extinction event. *Palaeogeography, Palaeoclimatology, Palaeoecology 252*, 132–144.

Wang, S. 1978: Late Permian and Early Triassic Ostracods of Western Guizhou and Northeastern Yunnan. *Acta Palaeontologica Sinica 17*, 47–138. [In Chinese with English abstract.]

Xiao, Y.F., Wu, K., Tian, L., Benton, M.J., Du, Y., Yang, H. & Tong, J.N. 2018: Framboidal pyrite evidence for persistent low oxygen content of shallow marine carbonates in the Nanpanjiang Basin during the Permian–Triassic transition. *Palaeogeography, Palaeoclimatology, Palaeoecology 511*, 243–255. Xie, S., Algeo, T.J., Zhou, W., Ruan, X., Luo, G., Huang, J. & Yan, J. 2017: Contrasting microbial community changes during mass extinctions at the Middle/Late Permian and Permian/Triassic boundaries. *Earth and Planetary Science Letters 460*, 180–191.

Wu, H., He, W. & Weldon, E.A. 2018: Prelude of benthic community collapse during the end-Permian mass extinction in siliciclastic offshore sub-basin: Brachiopod evidence from South China. *Global and Planetary Change 163*, 158–170.

Yang, H., Chen, Z., Wang, Y., Tong, J., Song, H. & Chen, J. 2011: Composition and structure of microbialite ecosystems following the end-Permian mass extinction in South China. *Palaeogeography, Palaeoclimatology, Palaeoecology 308*, 111–128.

Yin, H., Jiang, H., Xia, W., Feng, Q., Zhang, N. & Shen, J. 2014: The end-Permian regression in South China and its implication on mass extinction. *Earth-Science Reviews 137*, 19–33.

Yu, J.X., Broutin, J., Huang, Q. S. & Grauvogel, S. L. 2010: Annalepis, a pioneering lycopsid genus in the recovery of the Triassic land flora in South China. *Comptes Rendus Palevol 9*, 479–486.

Yuan, A., Crasquin, S., Feng, Q. & Gu, S. 2007: Latest Permian deep-water ostracods from southwestern Guangxi, South China. *Journal of Micropalaeontology 26*, 169–191.

Yuan, A.H. 2008: Latest Permian Deep-Water Ostracod (Crustacea) Fauna from South China. *University of Pierre & Marie Curie–China University of Geosciences (Wuhan)*, 240 pp.

Zhang, M., Jiang, H., Purnell, M.A. & Lai, X. 2017: Testing hypotheses of element loss and instability in the apparatus composition of complex conodonts: articulated skeletons of Hindeodus. *Palaeontology 60*, 595–608.

Zhu, X. 1999: Discoveries of the gastropods from the boundary bed at Yangou Section in Northeastern Jiangxi. *Journal of Jiangxi Normal University (Natural Science) 23*, 363–368. [In Chinese with English abstract.]

Figure Captions

Fig. 1. Palaeo-geographic maps of the global plates (A) and South China Block (B) during the Permian-Triassic transition. Map B shows the study section location (star) on the Yangtze Platform: YG = Yangou. The GSSP Meishan section is also marked by MS. The South China Block has rotated nearly 90° clockwise since the Permian-Triassic. Map A is adapted from Ron Blakey (http://jan.ucc.nau.edu/rcb7/), while map B is modified after Yin *et al*. (2014).

Fig. 2. A. Field photograph of the study section and ostracod-enriched intervals. B, C. Photographs of thin sections. Os = ostracods.

Fig. 3. Lithological, bio-stratigraphic and chemo-stratigraphic profiles of the study section. Conodont zonations are from Sun *et al*. (2012); Microfacies and carbon isotopes are from Tian *et al*. (2014a), MF-3: Algal and foraminiferal bioclastic sparitic limestone; MF-4: Coated-grain-bearing foraminiferal oolitic sparitic limestone; MF-5: Pyrite-bearing micritic limestone; MF-6: Dark shelly micritic limestone. Presented samples in this study are labelled by the narrows along the profiles.

Fig. 4. Ostracods of the Yangou section, part I. Scale bar width = 100 μm. A–D: *Hollinella* sp. 1, A, LY34+16i122, right lateral view, B, LY35+15i011, left lateral view, C, LY35+30i001, right lateral view, D, LY33+15i023, right lateral view; E–H: *Hollinella* sp. 2, E, LY35+10i011, right lateral view,

F, LY35+10i003, right lateral view, G, LY35+10i002, left lateral view, H, LY35+10i001, left lateral view; I–L: *Hollinella* sp. 3, I, LY36+0i012, right lateral view, J, LY36+0i005, right lateral view, K, LY36+0i013, left lateral view, L, LY36+0i003, left lateral view; M: *Langdaia suboblonga*, LY34+16i103, right lateral view; N–O: *Praezabythocypris ottomanensis*, N, LY34+16i093, right lateral view, O, LY34+28i051, right lateral view; P: *Langdaia* cf. *suboblonga*, LY34+16i052, left lateral view; Q–R: *Langdaia laolongdongensis*, Q, LY34+16i081, left lateral view, R, 34+16i052, right lateral view; S–T: *Langdaia* sp., S, LY34+16i053, right lateral view, T, LY34+28i127, right lateral view; U-V: *Paracypris gaetanii*, U, LY34+28i022, right lateral view, V, LY34+28i003, right lateral view; W-X: *Paracypris cf. gaetanii*, W, LY34+28i028, left lateral view, X, 34+28i003, right lateral view.

Fig. 5. Ostracods of the Yangou section, part Π. Scale bar width = 100 μm. A–B: *Praezabythocypris* cf. *ottomanensis*, A, LY34+16i116, right lateral view, B, LY34+16i047, left lateral view; C–D: *Acratia changxingensis*, C, LY34+16i047, right lateral view, D, LY34+16i056, left lateral view; E: *Liuzhinia* sp. 2, LY34+16i021, left lateral view; F: *Bairdia davehornei*, LY33+15i008, left lateral view; G–H: *Bairdia baudini*, G, LY34+16i064, left lateral view, H, 34+16i102, left lateral view; I–J: *Bairdia* sp. 1, I, LY34+28i006, right lateral view, J, LY34+28i030, right lateral view; K: *Bairdia* sp. 2, LY34+50i004, left lateral view; L–M: *Bairdiacypris* sp. 2, L, LY34+28i045, left lateral view, M, LY34+16i086, left lateral view; N–O: *Bairdiacypris* sp. 3, N, LY34+28i020, right lateral view, O, LY34+16i048, left lateral view; P: *Liuzhinia* cf. *antalyaensis*, LY34+28i045, right lateral view; Q–S: *Liuzhinia antalyaensis*, Q, LY34+28i031, right lateral view, R, LY34+28i059, left lateral view, S, LY34+28i058, left lateral view; T: *Liuzhinia* cf. *antalyaensis*, LY34+28i049, left lateral view; U:

527 *Liuzhinia* sp. 1, LY34+28i050, right lateral view; V: *Liuzhinia guangxiensis*, LY33+15i003, left
528 lateral view; W-X: *Bairdiacypris*? sp., W, LY34+16i060, left lateral view, X, LY34+16i037, left
529 lateral view.

530

531 **Fig. 6.** Height/Length diagram of the measured *Hollinella*.

532

533 **Fig. 7.** Faunal compositions of each study sample. Detailed data are in Table 1. Conodont zonations
534 are from Sun *et al*. (2012).

535

536 **Fig. 8.** Temporal size variations in the study samples. ETME = Earliest Triassic mass extinction.
537 Note, only one specimen is contained in the LY7 sample.

538

539 **Fig. 9.** Length/Height ratio distributions of the identified genera.

540

541

542

543 **Table 1**. Distributions of the identified ostracod taxa.

Taxa/Bed	LY1	LY2	LY3	LY4	LY5	LY6	LY7	LY8	LY9
Acratia changxingensis (Shi, 1987)		5							
Acratia sp.1		2		1					
Acratia sp.2		3		3					
Bairdia subsymmetrica (Shi, 1987)		5	2						
Bairdia cf. *subsymmetrica*		3	1	1					
Bairdia davehornei Forel et al., 2013	1								
Bairdia sp. 1		1	1	1					
Bairdia sp. 2		3	1						
Bairdia spp.				2				2	
Bairdiacypris anisica Kozur, 1971		5	1	1					
Bairdiacypris combeae Forel & Crasquin-Soleau, 2011		1	2						
Bairdiacypris sp.	2	2	6						
Bairdiacypris? sp.		3							
Hollinella sp.1	6	4		6		6	1	1	
Hollinella sp. 2					10	3			
Hollinella sp. 3								1	18
Langdaia laolongdongensis Crasquin-Soleau & Kershaw, 2005		12							
Langdaia cf. *laolongdongensis*		7	3						
Langdaia suboblonga Wang, 1978		6	1						
Langdaia cf. *suboblonga*		1	2						
Langdaia sp.	1	2							
Liuzhinia antalyaensis Crasquin-Soleau, 2004		8	15						
Liuzhinia cf. *antalyaensis*		3							
Liuzhinia guangxiensis Crasquin-Soleau, 2006	2	1	1						
Liuzhinia cf. *guangxiensis*		8	1						
Liuzhinia sp.1		1	2						
Liuzhinia sp.2			2						
Liuzhinia spp.		8	6						
Paracypris gaetanii Crasquin-Soleau, 2006		1	2						
Paracypris cf. *gaetanii*		2	1						
Paracypris sp.		3							
Praezabythocypris ottomanensis Crasquin-Soleau, 2004	1	3	4						
Praezabythocypris cf. *ottomanensis*	2	3	2						
Praezabythocypris spp.	1	2	1						

544

545 **Table 2. Ostracod faunal compositions of the detailed studied sections in different facies**

Paleo-geographic facies	Section name	Pre-LPME	PTTB	Post-ETME	References
Neritic clastic facies					
	Longchang	26 species of 15 genera	7 species of 4 genera	*	Hao 1992
	Zhongyin	21 species of 15 genera	5 species of 5 genera	*	Hao 1992
Non-microbialite shallow carbonate facies					
	Yangou	*	33 species of 8 genera	3 species of 2 genera	This study
	Bulla	54 species of 26 genera	15 species of 12 genera	*	Crasquin *et al*. 2008; Farabgoli *et al*. 2007
Microbialite-bearing shallow carbonate facies					
	Laolongdong	*	14 species of 8 genera	*	Crasquin & Kershaw 2005
	Chongyang	20 species of 5 genera	14 species of 7 genera	*	Liu *et al*. 2010
	Dajiang	17 species of 16 genera	10 species of 10 genera	*	Forel 2012
	Elikah River	56 species of 33 genera	29 species of 21 genera	*	Forel *et al*. 2015a
	Bükk Mountains	54 species of 16 genera	36 species of 15 genera	*	Forel *et al*. 2015b
	Çürük dag	28 species of 17 genera	12 species of 6 genera	*	Crasquin *et al*. 2004
Slope and deeper facies					
	Meishan	97 species of 25 genera	4 species of 4 genera	3 species of 3 genera	Crasquin *et al*. 2010
	Dongpan	48 species of 28 genera	8 species of 7 genera	*	Yuan *et al*. 2007

546 Footnote: * means no data. PTTB = Permian-Triassic transitional beds

547

548 Fig. 1

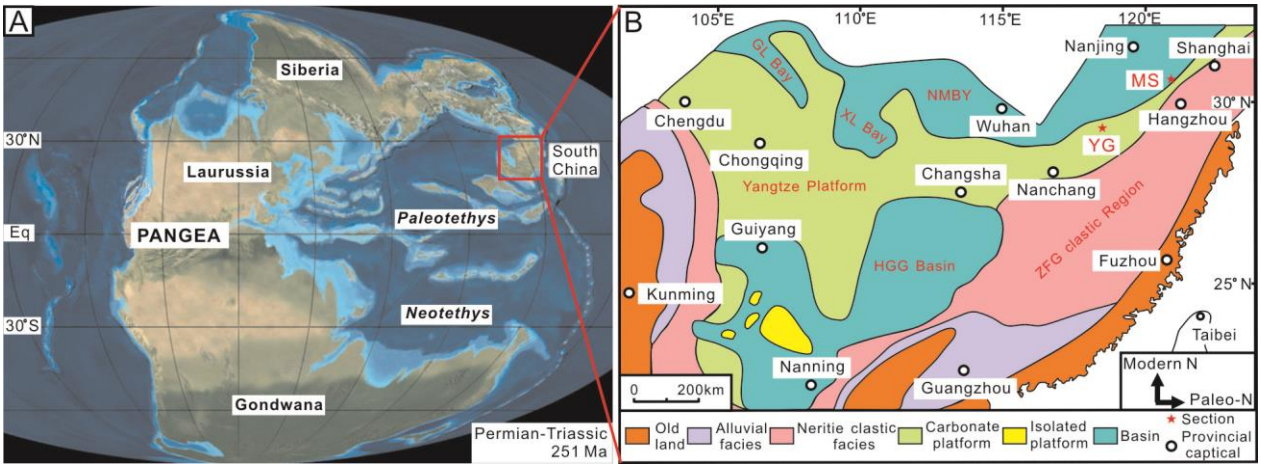

549

550

551 Fig. 2

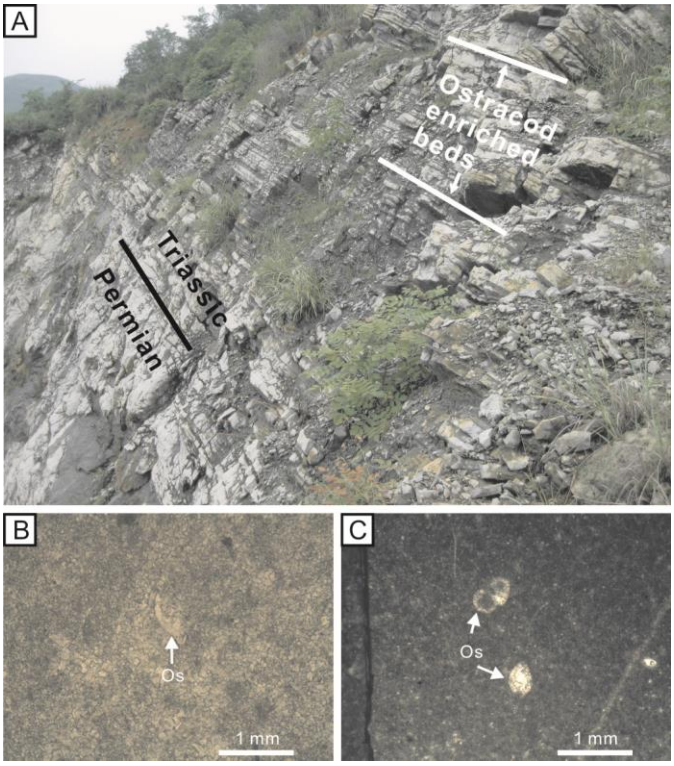

552

553

554

555 Fig. 3

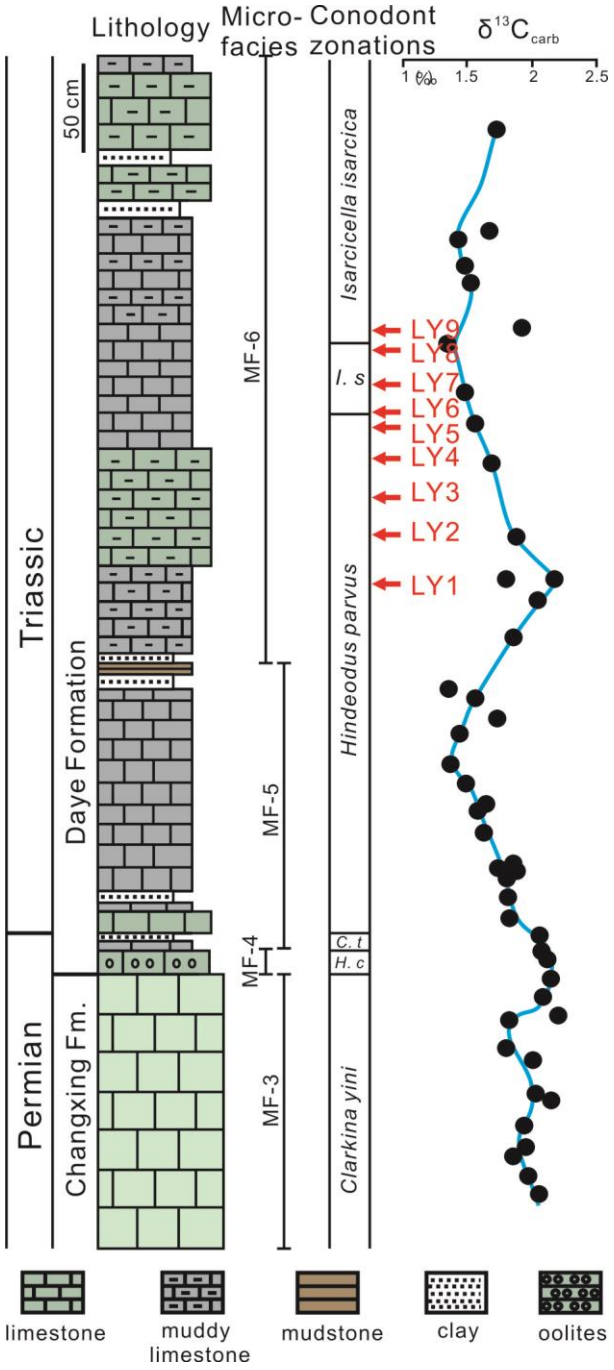

556

557

558

559 Fig. 4

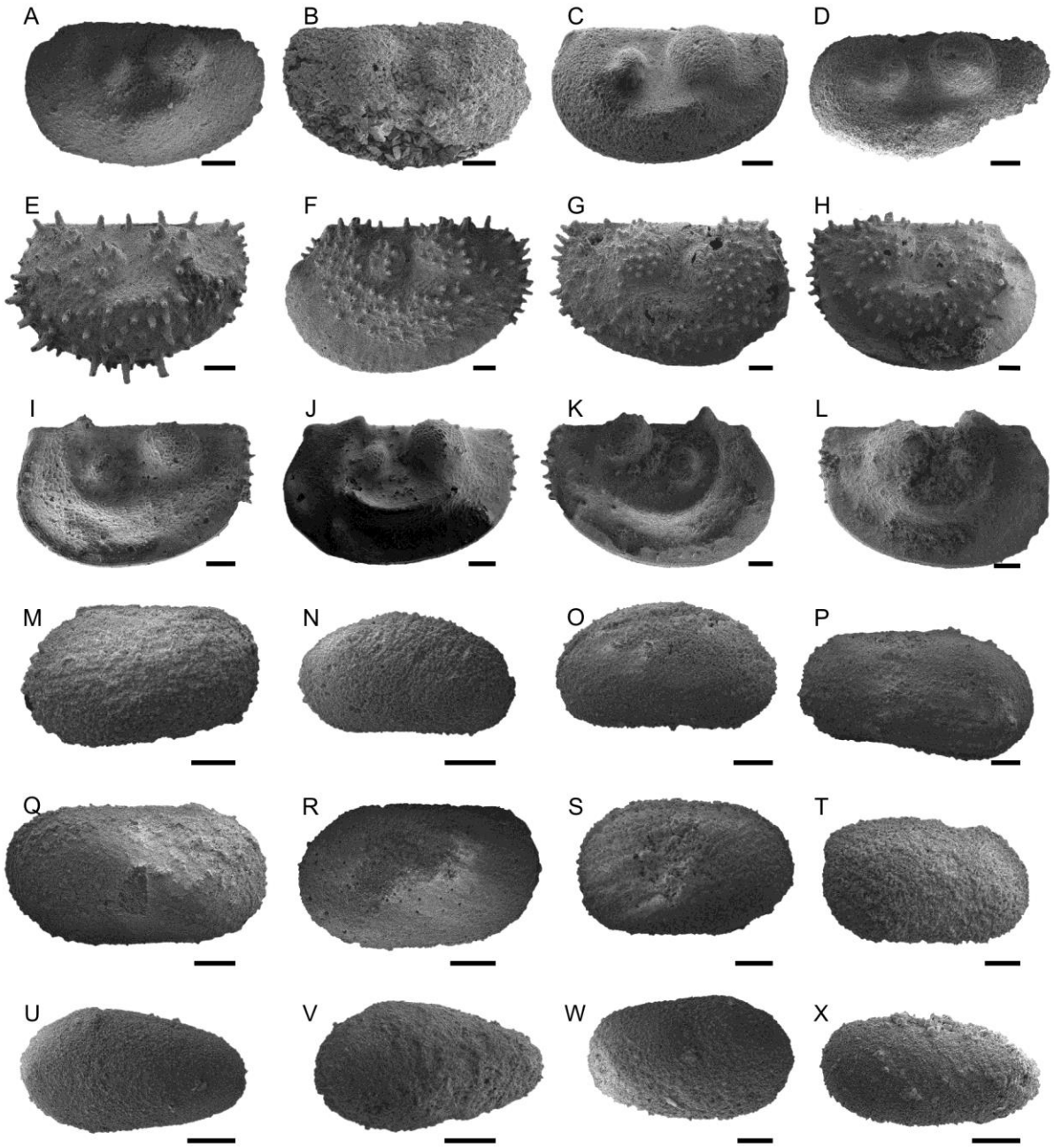

560

561

562

563 Fig. 5

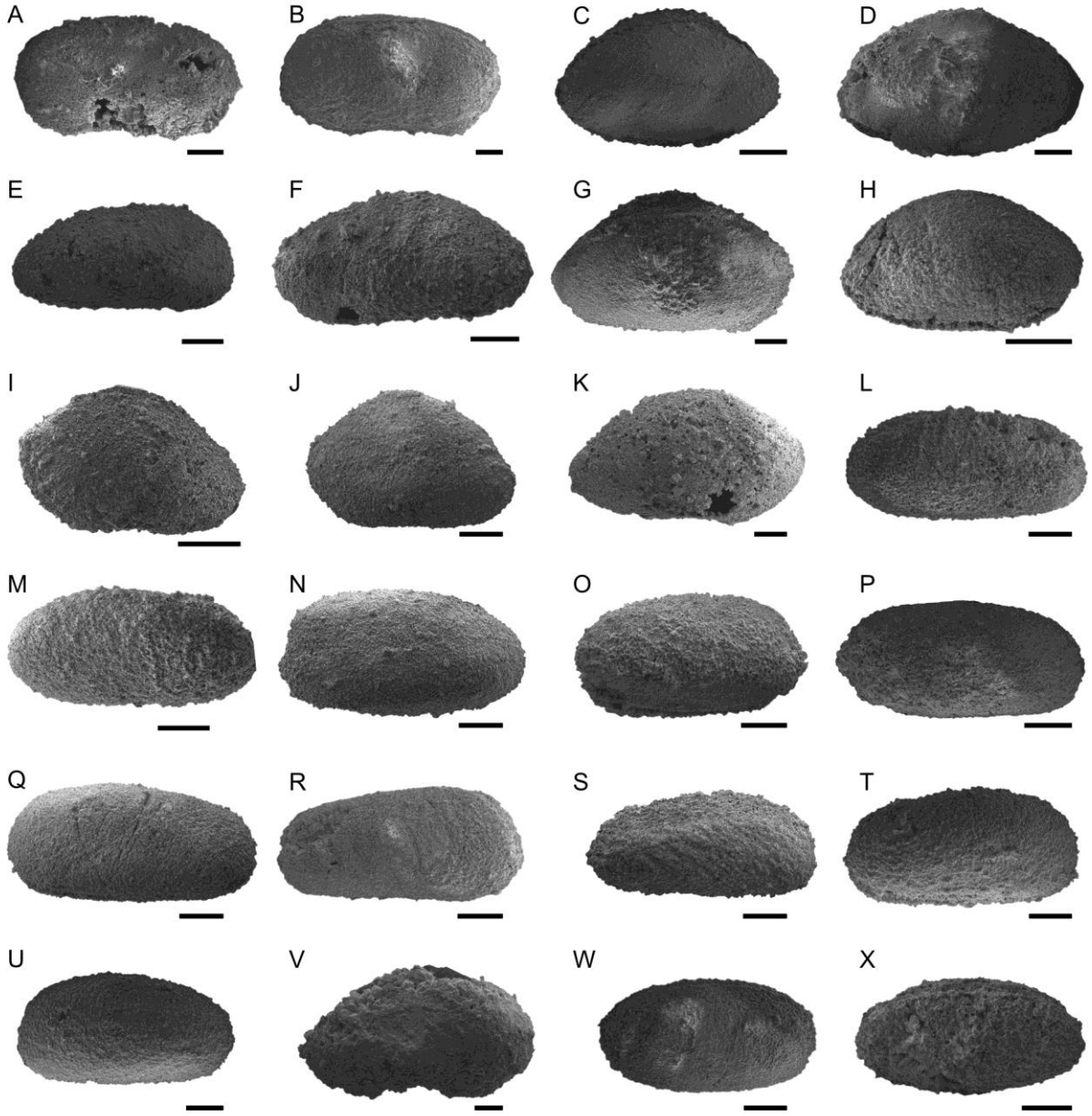

564

565

566 Fig. 6

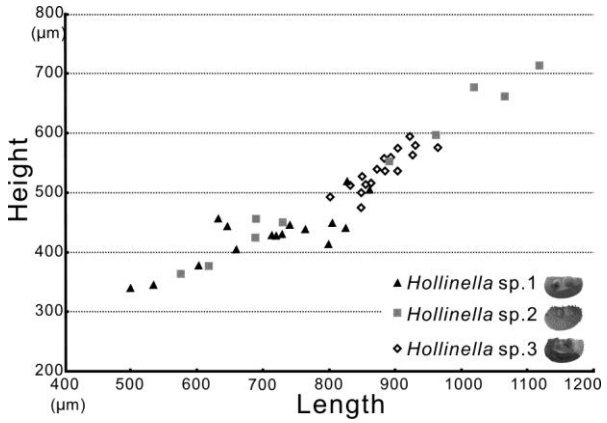

567

568

569 Fig. 7

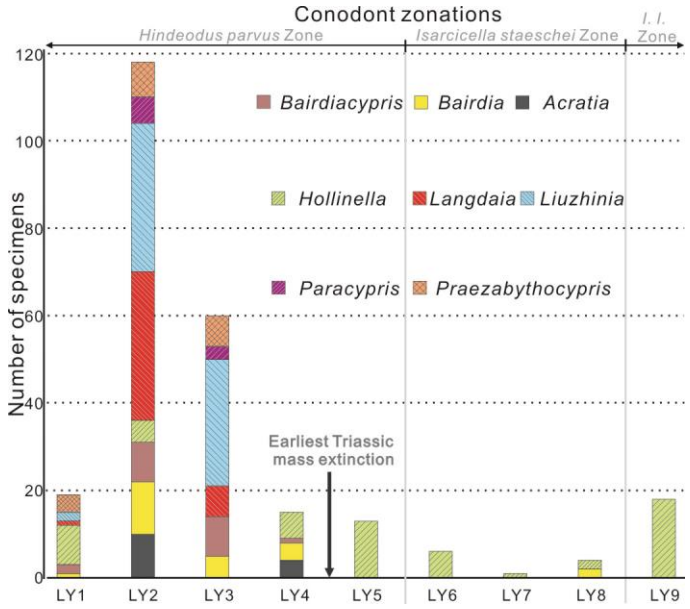

570

571

572

573 Fig. 8

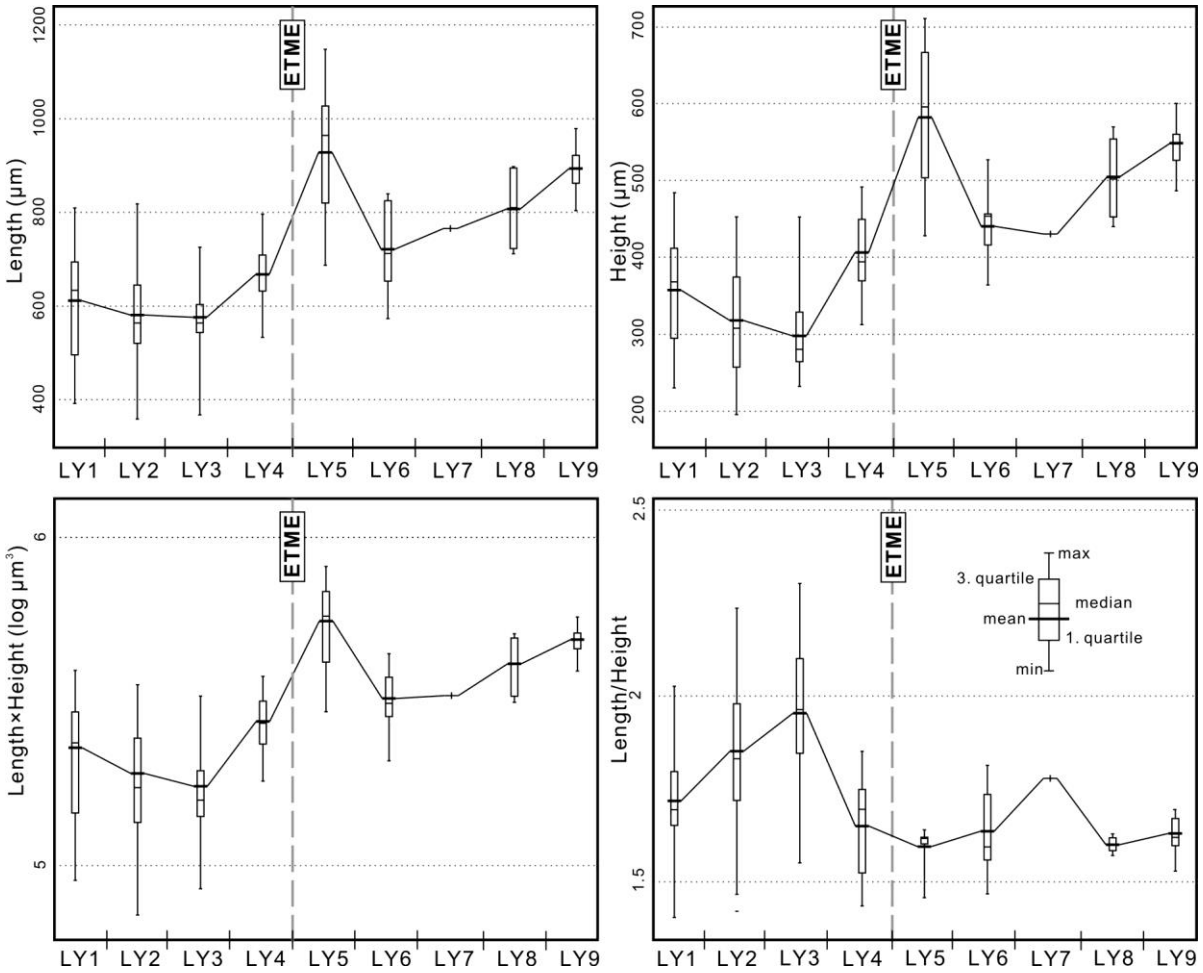

574

575

576 Fig. 9

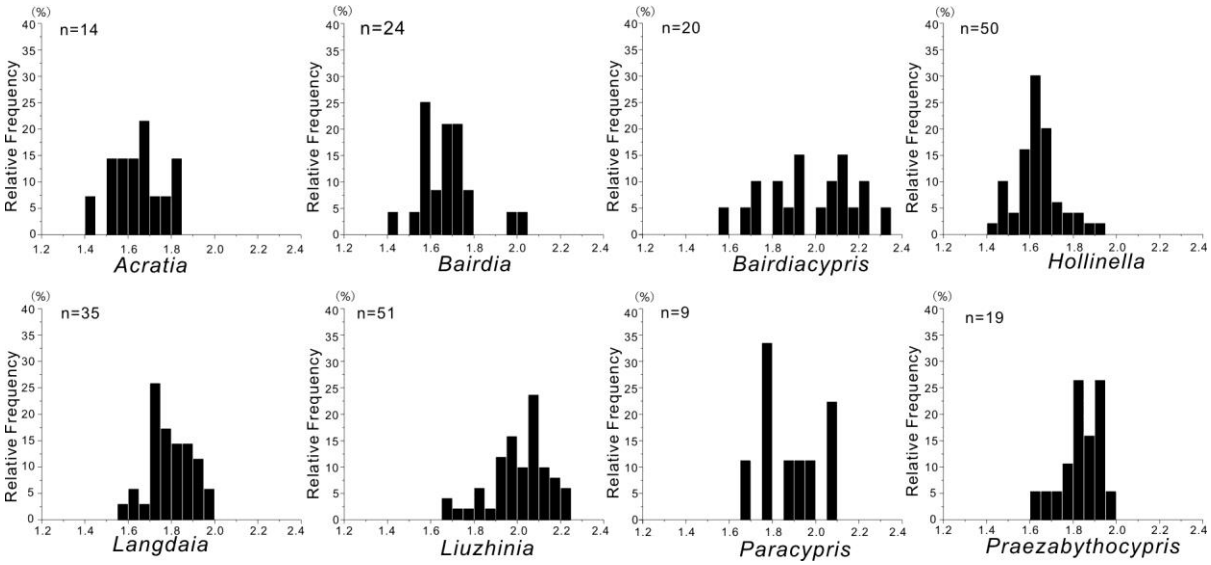

577